

Photochemical Mechanism of the Formation of Nanometer-Sized Copper by UV Irradiation of Ethanol Bis(2,4-pentandionato)copper(II) Solutions

Salvatore Giuffrida,* Guglielmo G. Condorelli, Lucia L. Costanzo, Ignazio L. Fragalà, Giorgio Ventimiglia, and Graziella Vecchio

Dipartimento di Scienze Chimiche, Università degli Studi di Catania and INSTM UdR di Catania, V.le A. Doria 6, Catania, Italy

Received August 22, 2003. Revised Manuscript Received December 23, 2003

The formation of colloidal metallic copper and of nanometer films on quartz and silicon substrates by irradiation of bis(2,4-pentanedionato)copper(II) ethanol solutions with UV light was investigated. The 254-nm-light absorption in the bulk of the solution causes formation of stable colloidal copper through two consecutive steps that could be distinguishable at low light intensity. In the first step, the starting complex releases one ligand and forms of copper(I) species that quickly release the second ligand and evolve to copper(I) alkoxides. In the second step, these latter undergo reduction to colloidal copper by the released acetylacetone with an electronic transfer process. Acetone sensitizes reduction to metallic copper with radical pathways. Features of the process depend on the acetone concentration so that either nanoparticles of colloidal copper or fine powder can be fabricated from the solution. In the presence of quartz or silicon substrate, placed in the suitable apparatus, the light absorption at the substrate–solution interface induces the formation of pure thin metallic copper films with nanometer characteristics. The photodeposition involves almost a heterogeneous process. The photoreaction has been followed by UV–vis and ^1H NMR spectroscopy while the copper(I) species have been detected by ESI-MS analysis and IR spectroscopy; copper powder and the films have been investigated by XRD, XPS, and SEM techniques. A mechanism of direct and acetone-sensitized formation of nanoparticles of copper is proposed, based on the role of the released ligand and on the photochemistry of the acetone.

Introduction

Nanoparticles of metals appear very promising from both fundamental and practical points of view because of their potentialities as functional materials in chemistry, physics, and biology. Various synthetic strategies have been, therefore, attempted in recent years to fabricate nanometer materials and thermal, photochemical, radiolytic, electrochemical, or sonochemical methods have been reported.^{1–9} Copper pure thin films are widely used as interconnect materials in multilevel integrated circuits because of the high conductivity and excellent electro migration resistance, whereas colloidal

nanoparticles have potential application in the heterogeneous catalysis and in nonlinear optical devices.

Laser ablation, thermal and photochemical reduction, and chemical vapor deposition (CVD) techniques have been used to obtain nanoparticles of metal and oxide.^{10–17}

In this paper, we report on the mechanism of a soft process well-suited for the synthesis of both colloidal copper and films in the nanometer scale, through irradiation of ethanol solution of the β -diketonate complex, bis(2,4-pentanedionato)copper(II) $[\text{Cu}(\text{acac})_2]$, which is commercially available. Some experimental results of this process have been reported in our recent communication.¹⁸ Note that the same molecule has been successfully used as a precursor in MOCVD^{17,19,20} and in photo-CVD²² to produce thin films of copper and

* To whom correspondence should be addressed. E-mail: sgiuffrida@dipchi.unict.it.

(1) Robertson, A.; Erb, U.; Palumbo, *Nanostruct. Mater.* **1999**, *12*, 1035–1040.

(2) Kometani, N.; Doi, H.; Asami K.; Yonezawa, Y. *Phys. Chem. Chem. Phys.* **2002**, *4*, 5142–5147.

(3) Roncoux, A.; Schulz J.; Patin, H. *Chem. Rev.* **2002**, *102*, 3757–3778.

(4) Yonezawa, Y.; Sato, T.; Ohno M.; Hada, H. *J. Chem. Soc., Faraday Trans. 1* **1987**, *83*, 1559–1567.

(5) Zhou, Y.; Wang, C.; Zhu Y. R.; Chen, Z. Y. *Chem. Mater.* **1999**, *11*, 2310–2312.

(6) Adair, J. H.; Li, T.; Kido, T.; Havey, K.; Moon, J.; Mecholsky, J.; Morrone, A.; Talham, D. R.; Ludwig M. H.; Wang, L. *Mater. Sci. Eng.* **1998**, *R23*, 139–242.

(7) Kruis, F. E.; Fissan, H.; Peled, *J. Aerosol Sci.* **1998**, *29*, 511–535.

(8) Rohrer, H. *Microelectron. Eng.* **1996**, *32*, 5–14.

(9) Krasnansky, R.; Yamamura S.; Thomas, J. K.; Dellaguardia, R. *Langmuir* **1991**, *7*, 2881–2886.

(10) Tsuji, T.; Iryo, K.; Nishimura Y.; Tsuji, M. *J. Photochem. Photobiol., A* **2001**, *145*, 201–207.

(11) Kapoor, S.; Palit D. K.; Mukherjee, T. *Chem. Phys. Lett.* **2002**, *355*, 383–387.

(12) Ohde, H.; Hunt F.; Wai, C. M. *Chem. Mater.* **2001**, *13*, 4130–4135.

(13) Huang, H. H.; Yan, F. Q.; Kek, Y. M.; Chew, C. H.; Xu, G. Q.; Oh, W.; Ji, P. S.; Tang, S. H. *Langmuir* **1997**, *13*, 172–175.

(14) Lisiecki, I.; Billoudet F.; Pileni, M. P. *J. Mol. Liq.* **1997**, *72*, 251–261.

(15) Yang, X. C.; Riehemann, W.; Dubiel, M.; Hofmeister, H. *Mater. Sci. Eng.* **2002**, *B95*, 299–307.

(16) Lin, D.; Wang, G. X.; Srivatsan, T. S.; Al-Hajri, M.; Petraroli, M. *Mater. Lett.* **2002**, *53*, 333–338.

(17) Nasibulin, A. G.; Ahonen, P. P.; Richard, O.; Kauppinen E. I.; Altman, I. S. *J. Nanopart. Res.* **2001**, *3*, 385–400.

copper oxide. The present methodology represents a friendly use simple technique which allows a fine modulation of copper colloid or film structural characteristics, depending on the experimental conditions adopted in the irradiation process.

Earlier studies^{23,24} have shown that irradiation of alcohol solutions of $\text{Cu}(\text{acac})_2$ at 254 nm results in reduction of copper(II) to copper metal, which forms a mirror on the irradiated cell wall. It has been proposed that the primary photochemical process consists of the reduction of $\text{Cu}(\text{acac})_2$ to $\text{Cu}(\text{acac})$, which undergoes thermal dismutation to copper(0) and $\text{Cu}(\text{acac})_2$. This mechanism is not consistent with the results obtained in our experimental conditions. Therefore, we have thoroughly investigated the photochemical processes occurring in the bulk of the solution as well as in the substrate–solution interface, taking into account the role of the released ligand. In fact, understanding of the entire process is a necessary step for adopting the photochemical process to produce nanometer copper.

Experimental Section

The bis(2,4-pentanedionato)copper(II) complex (C. Erba) was reagent grade and was sublimated prior to use. The acetylacetone (Hacac)(Merck) was distilled under vacuum prior to use. Anhydrous ethanol (C. Erba, % H_2O < 0.02) was spectrophotometric grade. The sodium salt of 2,9-dimethyl-4,7-diphenyl-1,10-phenanthroline disulphonic acid (BCDS) (Aldrich) has been used for copper(I) quantitative determination.

Ultraviolet–visible absorption spectra were measured with a Hewlett-Packard 8452A diode array and a Beckmann DU650 spectrophotometer. ^1H NMR spectra were recorded in $\text{C}_2\text{D}_5\text{OD}$ on a Variant INOVA 500-MHz instrument with a 5-mm quartz tube. Electron spin resonance spectroscopy (ESR) was carried out with a Bruker ESP 3220 spectrometer. X-ray photoelectron spectroscopy (XPS) measurements were performed with a PHI 5600 Multy Technique System adopting a standard Mg X-ray source and an electron takeoff angle of 45° . To prevent any possible oxidation, products of solution photoreaction (powders and films) were handled under a nitrogen atmosphere and quickly introduced into the XPS chamber (10^{-10} Torr). Powders were obtained from evaporation on silicon substrates of reacted solutions. Spectra have been quickly collected for a few minutes for each sample to avoid unwanted X-ray-induced reduction of the sample. Binding energy (B.E.) shifts, hence reduction effects, were not observed during measurements. B.E. data have been calibrated on “adventitious” C 1s at 285 eV.^{25,26} Depth profiles were obtained by alternating sputter etching rastered over a 3×3 mm area (with a 4-kV argon ion gun) and XPS analysis. X-ray diffraction measurements (XRD) were made on powders precipitated from colloidal solutions using a Bruker AXS D5005 X-ray diffractometer equipped with a copper anode and an attachment for thin film measurements. $20^\circ < 2\theta < 70^\circ$ detector scans were

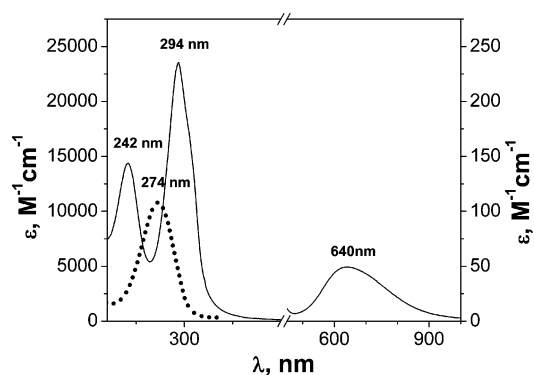


Figure 1. Electronic spectra in ethanol solution: $\text{Cu}(\text{acac})_2$ (—) and Hacac (···).

adopted. Electrospray ionization mass spectrometry (ESI-MS) was performed using a Finnigan LCQ^{duo} (thermoquest) instrument. Fourier transform infrared spectroscopy (FT-IR) analysis was performed with a FT/IR 430 Jasco spectrometer. Powder samples were analyzed in KBr pellets. Spectra were recorded in the $450\text{--}4500\text{-cm}^{-1}$ spectral region. The resolution was 4 cm^{-1} .

All the experiments were carried out with $\text{Cu}(\text{acac})_2$ ($0.5\text{--}5 \times 10^{-4}$ mol L^{-1} solutions, in a N_2 atmosphere at 25°C . Spectrophotometric 1×3 cm cuvettes have been generally used. Irradiation has been performed in the spectrophotometric cuvettes or in quartz tubes using a Rayonet photochemical reactor, equipped with various numbers of lamps with monochromatic emission at either 254 nm or at 300 nm. The light intensity, measured by a ferric oxalate actinometer,²⁷ was in the range of 2.0×10^{-6} to 1.0×10^{-5} $\text{N}h\nu\text{ min}^{-1}$ ($5\text{--}27\text{ mW cm}^{-2}$).

Film deposition from the solution irradiated in the presence of quartz or Si(100) substrates has been performed in a suitable apparatus described in detail in the Results and Discussion section. ^1H NMR spectra of irradiated solutions have been measured to identify photoproducts using quartz tube containing deaerated solution at various times of irradiation. Preliminary experiments have shown that addition of $\text{Cu}(\text{acac})_2$ does not affect NMR signals of both the solvent and of the exogenous Hacac. In fact, $\text{Cu}(\text{acac})_2$ in d_6 -ethanol did not show any signal of the bounded acac^- ; the spectra of Hacac, performed in the presence of $\text{Cu}(\text{acac})_2$, maintained unaltered the chemical shift and the sharpness of the signals. This suggested that the exchange rate of the ligand of $\text{Cu}(\text{acac})_2$ was very slow.

The concentration of copper(I) in the irradiated solution has been evaluated by the absorbance of $\text{Cu}^{\text{I}}(\text{BCDS})$ upon addition of BCDS under N_2 ($\lambda_{\text{max}} = 480\text{ nm}$, $\epsilon = 14000$ in $\text{C}_2\text{H}_5\text{OH}$).²⁸ BCDS reacts very fast with the copper(I) photochemical intermediate with a pseudo first-order kinetics ($k_{\text{obs}} = 0.018\text{ s}^{-1}$). Possible errors in copper(I) determinations are negligible in present experimental conditions. There is, in fact, evidence that the starting compound reacts with BCDS very slowly ($k_{\text{obs}} = 6.11 \times 10^{-6}\text{ s}^{-1}$) because the equilibrium $\text{Cu}^{\text{II}} \rightleftharpoons \text{Cu}^{\text{I}}$ is greatly shifted toward the left. Besides, several parallel ESR experiments have shown that after irradiation the lowering of the initial $\text{Cu}(\text{acac})_2$ concentration exactly complements the copper(I) concentration determined by the BCDS method.

Deaerated $\text{Cu}(\text{acac})_2$ ethanol solutions have also been irradiated at 300 nm upon adding acetone ($0.01\text{--}0.1\text{ mol L}^{-1}$).

Results and Discussion

Electronic Spectra. The electronic absorption spectra of Hacac and $\text{Cu}(\text{acac})_2$ in anhydrous $\text{C}_2\text{H}_5\text{OH}$ are compared in Figure 1.

(18) Condorelli, G. G.; Costanzo, L. L.; Fragalà, I. L.; Giuffrida, S.; Ventimiglia, G. *J. Mater. Chem.* **2003**, *13*, 2409–2411.

(19) Condorelli, G. G.; Malandrino G.; Fragalà, I. *Chem. Mater.* **1995**, *7*, 2096–2103.

(20) Condorelli, G. G.; Malandrino G.; Fragalà, I. *Chem. Vap. Deposition* **1999**, *5*, 21–27.

(21) Chiang, C.; Miller, T. M.; Dubois, L. H. *J. Phys. Chem.* **1993**, *97*, 11781–11786.

(22) Maury, F.; Vidal S.; Gleizes, A. *Adv. Mater. Opt. Electron.* **2000**, *10*, 123–133.

(23) Marciniak B.; Buono-Core, G. E. *J. Photochem. Photobiol., A* **1990**, *52*, 1–25, and references therein.

(24) Marciniak, B.; Hug, G. L. *Coord. Chem. Rev.* **1997**, *159*, 55–74.

(25) Teterin, Y. A.; Sosulnikov, M. I. *Physica C* **1993**, *212* (3–4), 306–316.

(26) Swift, P. *Surf. Interface Anal.* **1982**, *4* (2), 47–51.

(27) Calvert, J.; Pitts, J. N. In *Experimental Methods in Photochemistry*; John Wiley and Sons: New York, 1966; p 783.

(28) Žak, B. *Clin. Chim. Acta* **1958**, *3*, 328–334.

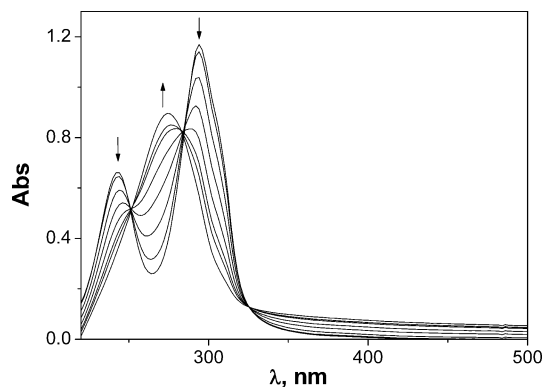


Figure 2. Spectral changes upon irradiating $\text{Cu}(\text{acac})_2$ in ethanol solution at 254 nm at various times (0–65'). $[\text{Cu}(\text{acac})_2] = 0.5 \times 10^{-4} \text{ mol L}^{-1}$, $Nh\nu = 2 \times 10^{-6} \text{ einstein min}^{-1}$ (5 mW cm^{-2}).

The single band at 274 nm ($\epsilon = 11000$) in the Hacac solution is consistent with a $\pi\text{--}\pi^*$ (HOMO \rightarrow LUMO) transition.²⁹ Beyond 220 nm, the $\text{Cu}(\text{acac})_2$ spectrum displays three distinct bands at 242 nm ($\epsilon = 14500$), at 294 nm ($\epsilon = 23500$), and 640 nm ($\epsilon = 50$).

Previous spectroscopic studies^{30–33} pointed out that the strong band at 242 nm represents the LMCT transition while the intense band at 294 nm is assigned to the two π_{L} to π^*_{L} transitions (IL). The band centered at 640 nm represents the copper(II) d–d ligand field transitions.

Photochemical Formation of Colloidal Copper.

Irradiation of deoxygenated ethanol solutions of $\text{Cu}(\text{acac})_2$ at 254 nm causes spectral changes consisting of a decrease of the absorption bands at 242 and 294 nm, appearance of a new band at 274 nm, and a slight increase of absorbance over 326 nm (Figure 2). In the visible region a broad maximum at about 620 nm, responsible for the pale-green coloration of the irradiated solution, becomes detectable. The spectral patterns show three isosbestic points, at 252, 285, and 326 nm (Figure 2). The isosbestic points at 252 and 285 nm are consistent with a photochemical reaction involving release of both the Hacac ligands and formation of copper species which do not absorb in that spectral region, whereas the isosbestic point at 326 nm indicates that these species absorb at longer wavelengths.

The release of free acetylacetone during the photochemical reaction is also evidenced by ^1H NMR measurements. In Figure 3 the spectra of $\text{Cu}(\text{acac})_2$ solution, before and after 120 and 240 min of irradiation, are shown. There is evidence of signals due to Hacac methyl groups of both keto and the enolic tautomers, at 2.19 and 2.02 ppm. The free Hacac concentration increases with the irradiation time. The signals of the methylenic protons of keto and enolic Hacac are not well evident because of the low concentration of the sample. There

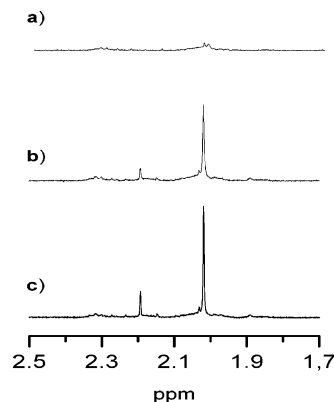


Figure 3. NMR spectra of $\text{Cu}(\text{acac})_2$ ($10^{-4} \text{ mol L}^{-1}$) in $\text{C}_2\text{D}_5\text{OD}$ at different times of irradiation, in a quartz tube: (a) $t_{\text{irr}} = 0$; (b) $t_{\text{irr}} = 120 \text{ min}$; (c) $t_{\text{irr}} = 240 \text{ min}$.

are no signals attributable to any acac^- bound to copper(I), thus ruling out the $\text{Cu}(\text{acac})$ presence in solution.

On continuing the irradiation, the isosbestic points shift, thus indicating that a new reaction is occurring. Besides, the deep green solution turns to wine red, whereas the absorption maximum at 620 nm shifts to about 575 nm, which is the characteristic region of the plasmon peak of copper metal in the colloidal state.^{13,34} These observations allow us to take into consideration two successive steps of photoreaction, respectively, before and after the shift of the isosbestic points.

Low-intensity irradiation of less concentrated solutions ($\leq 10^{-4} \text{ mol L}^{-1}$) results in constant isosbestic points and yields a maximum value of absorbance at 274 nm. This value matches that expected for completely released Hacac. In these conditions first and second steps are sharply distinguishable.

In more concentrated solutions ($> 10^{-4} \text{ mol L}^{-1}$), the isosbestic points shift before the complete ligand release and, therefore, the two steps are overlapping.

Methanol solutions irradiated in the same conditions show the same photochemical behavior as found in ethanol solutions.

Experiments performed with light at 300 nm proved that the $\text{Cu}(\text{acac})_2$ is unreactive at this wavelength according to previous literature.²³

First Step of Reaction: Ligand Release and Formation of Copper(I) Species. In the first step of the photoreaction, the formation of copper(I) species and the release of the free ligand occur without any detectable side reactions. The copper(I) species have been qualitatively and quantitatively identified by the addition of excess of solid BCDS, a specific reagent for copper(I)²⁸ that yields the CuBCDS complex, with an absorption maximum at 480 nm. The quantum yield of the disappearance of copper(II), equal to copper(I) formation one, is $\phi_{\text{Cu}} = 5 \times 10^{-3}$. It was determined with solutions $10^{-4} \text{ mol L}^{-1}$ and light intensity of $2.0 \times 10^{-6} N h \nu \text{ min}^{-1}$ (5 mW cm^{-2}).

In all experiments, the complete back reaction can be achieved upon interruption of the irradiation and saturation with air. No side reactions are evident. There is, therefore, evidence that no sizable photodegradation of the released ligand occurs.

(29) Nakanishi, H.; Morita, H.; Nagakura, S. *Bull. Chem. Soc. Jpn.* **1977**, *50*, 2255–2261.

(30) Cotton, F. A.; Wise, J. J. *Inorg. Chem.* **1967**, *6* (5), 915–916.

(31) Belford, R. L.; Carmichael, J. W., Jr. *J. Chem. Phys.* **1967**, *46*, 4515–4522.

(32) Yokoi, H. *Inorg. Chem.* **1978**, *17*, 538–542.

(33) (a) Tsiamis, C.; Cambenis S.; Halgikostos, C. *Inorg. Chem.* **1987**, *26*, 26–32. (b) Tsiamis, C.; Michael, C.; Jannakoudais A. D.; Jannakoudais, P. D. *Inorg. Chim. Acta* **1986**, *120* (1), 1–9, and references therein.

(34) Yeh, M. S.; Lee, Y. S. Y. P.; Lee, H. F.; Yeh, Y. H.; Yeh, C. S. *J. Phys. Chem. B* **1999**, *103*, 6851–6857.

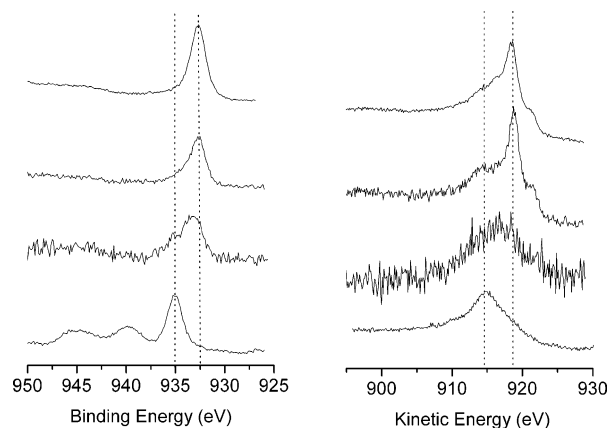


Figure 4. XPS spectra of (a) $\text{Cu}(\text{acac})_2$ powders on Si; (b) copper(I) solution (first step) evaporated on Si; (c) copper powder on Si obtained after the second step; (d) copper film on quartz. Cu $2p_{3/2}$ (left) and Cu LMM (right) regions.

ESI mass spectrometry has been adopted to investigate the nature of copper species present in the first reaction step. All tests have used solutions up to 10^{-4} mol L^{-1} irradiated until the occurrence of a complete ligand release. In these conditions the copper(I) concentration is identical to that of the initial $\text{Cu}(\text{acac})_2$.

ESI mass spectra show the characteristic copper pattern distribution that can fit either to monomer or to dimer copper(I) ethoxide: m/z 123 [$\text{Hacac} + \text{Na}$] $^+$, m/z 193 [$\text{Cu}(\text{OC}_2\text{H}_5)(\text{C}_2\text{H}_5\text{OH}) + \text{K}$] $^+$, m/z 347 [$\text{Cu}_2(\text{OC}_2\text{H}_5)_2(\text{C}_2\text{H}_5\text{OH})_2 + \text{K}$] $^+$, and m/z 458 [$\text{Cu}_2(\text{C}_2\text{H}_5\text{O})_2(\text{Hacac})_2 + \text{H}_2\text{O} + \text{Na}$] $^+$.

Further ESI mass experiments with methanol solutions, irradiated up to the complete ligand release, give peaks with the similar copper pattern at m/z 123 [$\text{Hacac} + \text{Na}$] $^+$, m/z 165 [$\text{Cu}(\text{OCH}_3)(\text{CH}_3\text{OH}) + \text{K}$] $^+$, and m/z 412 [$\text{Cu}_2(\text{OCH}_3)_2(\text{Hacac})_2 + \text{Na}$] $^+$ as expected for the parent methoxide.

The formation of copper(I) species has also been confirmed by XPS analysis of a film obtained upon evaporation on a Si(100) substrate of some drops of the solution, irradiated until the complete ligand release, under vacuum and nitrogen flux. This spectrum is compared to that of the presence of reference $\text{Cu}(\text{acac})_2$ powders in Figure 4.

The Cu $2p_{3/2}$ photoelectron signal consists of two peaks (Figure 4b). The higher B.E. feature at 935 eV can be assigned either to unreacted $\text{Cu}(\text{acac})_2$ or to superficial copper(II) hydroxide.^{35,36} The remainder at 933 eV is certainly due to the copper(I) photoproduct. There is no evidence of any relevant shake-up band in the 937–947-eV region, thus ruling out any copper(II) compound as the main reaction product. Moreover, the kinetic energy value (916.7 eV) of the Cu LMM Auger signal does not fit either the metallic copper (918.6 eV) or Cu_2O (916 eV). Hence, it can be safely assigned to copper(I) photoproduct.^{19,36}

Furthermore, the UV–vis spectra of the irradiated solutions exhibit evidence of agglomeration effect since they show a band at 620 nm, typical of colloidal copper-

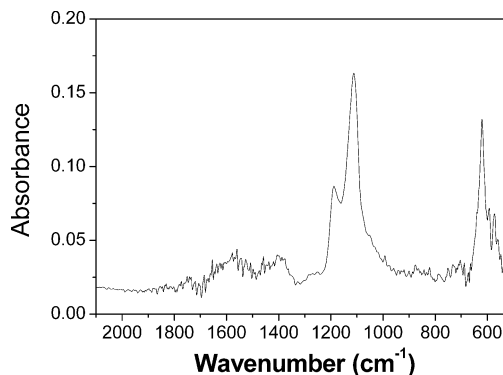


Figure 5. FT-IR spectrum of the precipitate obtained after aging of the first step solution.

(I) species.³³ In accordance with the literature,³⁷ this observation can be associated to copper(I) oligomer alkoxide.

No thermal dismutation of the colloidal copper(I) was observed. In fact, after aging in the dark for about 12 h in the absence of oxygen, the colloidal solutions give a deep green precipitate that reacts completely with BCDS, indicating that it consists mainly of copper(I) species.

XRD analysis of this precipitate does not show any significant peak, thus suggesting the absence of metallic copper.

Moreover, IR spectra show that it consists mainly of $\text{Cu}(\text{OC}_2\text{H}_5)$. The spectra, in fact, exhibit three main bands at 625, 1120, and 1200 cm^{-1} . The first falls in the region of M–O stretches of metal alkoxides³⁸ while the others can be assigned to C–O alkoxide stretches (Figure 5). Broad bands around 1580 and 1430 cm^{-1} can be assigned to $\nu(\text{C}=\text{C}, \text{C}=\text{O})$ and $\delta(\text{CH}) + \nu(\text{C}=\text{O})$ vibration of residual $\text{Cu}(\text{acac})_2$.³⁸

Further irradiation of the colloidal copper(I) solutions leads to copper(0) formation, thus proving that the reduction is photoinduced.

Second Step: Formation of Colloidal Copper. To best monitor photoreduction to copper(0) occurring in the second step, more concentrated ($>10^{-4}$ mol L^{-1}) solutions have been used. In these conditions, the two steps are overlapped. The formation of copper nanoparticles has been followed through the plasmon absorption at about 574 nm, which increases upon irradiation until a maximum value (Figure 6a). The peak wavelength, which is associable to the particle dimensions,³⁹ falls in the range 570–580 nm, depending on light intensity, thus on the formation rate. For example, if the conditions reported in Figure 6a are varied, the peak at 574 nm moves to shorter wavelengths, by increasing the incident light intensity. In contrast, it shifts to longer wavelengths by decreasing the light intensity. In all cases, prolonged irradiation causes a broadening of the band, a shift toward the visible, and a decreasing of the peak intensity, likely due to the agglomeration of particles.

(37) Mehrotra, R. C.; Singh, A. In *Progress in Inorganic Chemistry*; John Wiley and Sons Inc.: New York, 1997; Vol. 46.

(38) Nakamoto, K. In *Infrared and Raman Spectra of Inorganic and Coordination Compounds*; John Wiley and Sons Inc.: New York, 1978; pp 230 and 249.

(39) Creighton, J. A.; Eadon, D. G. *J. Chem. Soc., Faraday Trans. 1991*, 87 (24), 3881–3891.

(35) Badrinarayan, S.; Mandale A. B.; Sainkar, S. R. *J. Mater. Res.* 1996, 11, 1605–1608.

(36) Wagner, C. D. In *Practical Surface Analysis Vol. 1*; Briggs, D., Seah, M. P., Eds.; John Wiley and Sons Ltd: Chichester, England, 1995; p 608.

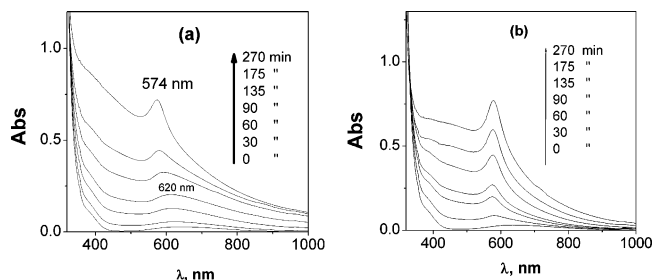


Figure 6. Spectral changes in the visible region upon irradiating $\text{Cu}(\text{acac})_2$ [$\text{Cu}(\text{acac})_2$] = 5×10^{-4} mol L^{-1} in ethanol solution at 254 nm at various times, $Nh\nu = 5 \times 10^{-6}$ einstein min^{-1} (27 mW cm^{-2}), (a) in the absence of free Hacac and (b) with addition of Hacac (10^{-3} mol L^{-1}).

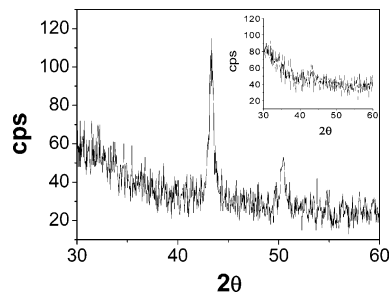


Figure 7. XRD pattern of the precipitate obtained from 2^o step. Inset: XRD profile of the precipitate obtained from 1^o step.

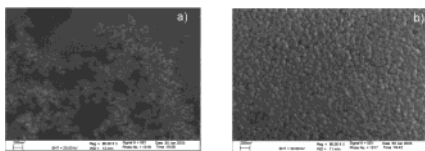


Figure 8. SEM micrographs of copper powders obtained in the second step (a) and of a copper film on quartz (b).

The formation of copper nanoparticles has also been proved by XPS, XRD, and SEM analyses.

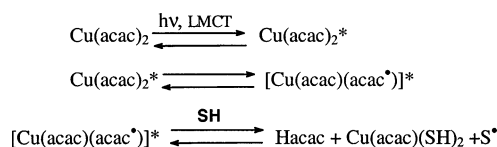
XPS spectra of Cu powders, dried on a silicon substrate, are reported in Figure 4c. The shapes and positions of the Cu 2p_{3/2} photoelectron peak (B.E. = 932.6 eV) and of the Cu LMM Auger band (KE = 918.6 eV) are consistent with the presence of metallic copper.³⁶ XRD pattern of the powders (Figure 7) similarly shows the reflections, (111) and (200), of metallic copper while SEM micrographs of dried powders show nanodimensioned grains with an average size of about 50 nm (Figure 8a).

The colloidal solution of copper, in an inert atmosphere, remains stable for about 48 h. Longer aging causes the broadening of the band to longer wavelengths, the decreasing of the intensity of the plasmon absorption, and the formation of a fine precipitate. Saturation with air reversed the reaction and colloidal copper is back-transformed to $\text{Cu}(\text{acac})_2$.

Irradiation of 5×10^{-4} mol L^{-1} solution results in the formation of copper(0) thin film on the cuvette walls and, in turn, in the attenuation of the intensity of the incident light.

Photoreduction Mechanism. Photoreduction of $\text{Cu}(\text{acac})_2$ to copper(I) occurs by irradiation of the ligand-to-metal charge-transfer band (LMCT). This causes the homolytic cleavage of Cu–O bond and the formation of the acetylacetononyl radical that abstracts one hydrogen

Scheme 1



atom from solvent, thus competing with the reverse electron transfer (Scheme 1):²³

SH represents a hydrogen-atom-donating solvent and the S^\bullet radical can decay through dismutation to aldehyde and alcohol.

The $\text{Cu}(\text{acac})$ complex has not been detected in the NMR spectra. Nevertheless, it can be an intermediate, which undergoes fast alcoholysis by the coordinated solvent molecules to the ethoxide species found in the ESI mass spectra. These latter quickly undergo oligomerization with formation of colloidal species responsible for absorption at about 620 nm.

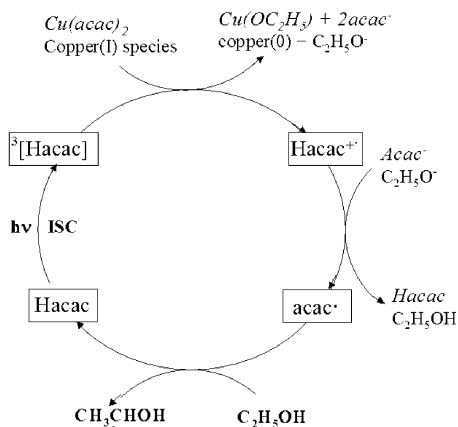
In the adopted conditions, there is no evidence of any thermal dismutation process. By contrast, there is clear evidence of a photoinduced reduction that is likely sensitized by the released Hacac ligand since it represents the only species absorbing at 254 nm in the copper(I) solution. Two significant experiments provide support for this observation. A 5×10^{-4} mol L^{-1} $\text{Cu}(\text{acac})_2$ solution (a) and a 5×10^{-4} mol L^{-1} $\text{Cu}(\text{acac})_2$ – 10^{-3} mol L^{-1} Hacac solution (b) have been simultaneously irradiated at 254 nm. In these conditions, the fraction of the light absorbed by the initial complex is 100% in the sample (a) and 40% in the sample (b). The kinetics of the formation of copper(0) can be measured through the intensity of the copper plasmon absorption at 574 nm. The rate is almost equal in both samples (Figure 6, a and b). This proves that the Hacac works as a sensitizer rather than a filter. Besides, the lack of the broad band at 620 nm in the sample (b) is consistent with a fast reduction of copper(I) species to copper(0).

In the second experiment, both samples (a) and (b) have been irradiated at 300 nm. After some hours, the plasmon peak at about 574 nm is evident in sample (b), whereas, as expected, no spectral changes occur in sample (a). These results indicate that Hacac sensitizes the reduction of copper(II) and copper(I) species to metallic copper.

It has been demonstrated (vide supra) that the air saturation of the photoreacted solutions causes back reaction to $\text{Cu}(\text{acac})_2$ in a concentration almost equal to the initial value, without any addition of Hacac. This observation suggests that sensitization does not involve byproducts of the released ligand. Probably it involves an electron-transfer process in which the Hacac triplets, formed by the irradiation, transfer an electron to copper(II) and/or copper(I) species with a following reduction to copper(0) (Scheme 2).

Photoreduction of $\text{Cu}(\text{acac})_2$ Sensitized by Acetone. The irradiation at 300 nm of ethanol solutions of $\text{Cu}(\text{acac})_2$ in the presence of acetone causes reduction to copper(0). At low concentration of acetone (0.01 mol L^{-1}), the spectral variations of the $\text{Cu}(\text{acac})_2$ exactly match those observed in the direct photoreaction, namely, a broad absorption at 620 nm that shifts to about 580 nm with the irradiation time. Upon increasing the acetone concentration, a broad band without a well-

Scheme 2. Proposed Mechanism for the Photoreduction of Cu(acac)₂ Sensitized by Hacac



defined maximum appears in the visible region and precipitation of a dark powder occurs within a few minutes.

For example, a dark powder is formed within 15 min by irradiating a 5×10^{-4} mol L⁻¹ Cu(acac)₂/0.1 mol L⁻¹ acetone solution with light of 2.5×10^{-6} N/hv min⁻¹ (5.5 mW cm⁻²). The powder, collected by decanting or centrifugation in an inert atmosphere, has been analyzed with XRD and XPS techniques. Both analyses show that it consists of metallic copper.

The present results are consistent with a sensitized radical mechanism (Scheme 2) involving the reduction of Cu(acac)₂ to copper(I) species, which, in turn, can be reduced to metallic copper through ketyl and/or ethanol radicals, due to the acetone photodegradation.⁴⁰ To understand which radical is reactive toward the Cu^{II(I)} → Cu^{I(0)} reduction, two different experiments have been carried out. A 5×10^{-4} mol L⁻¹ Cu(acac)₂ ethanol solution has been irradiated at 300 nm in the presence of *tert*-butyl peroxide (BuOOBu). In this case, the BuO• radicals⁴¹ cause H• abstraction from C₂H₅OH and Cu^{II} → Cu⁰ reduction is observed. In the second experiment a solution of Cu(acac)₂ (5×10^{-4} mol L⁻¹) and acetone (0.01 mol L⁻¹) in 2-propanol has been irradiated. In this case, the (CH₃)₂C=O triplet abstracts a hydrogen atom from the solvent⁴² and both acetone and solvent give the same ketyl radical. Also in this case, reduction reaction occurs, thus showing that both ketyl and ethanol radicals are reductive agents for copper(II) and copper(I).

The rate of the two reductive steps depend on the concentration of formed radicals. Copper(0) colloidal solutions are formed at a reaction rate comparable to direct process, while copper(0) precipitate can be obtained at greater reaction rates.

Formation of the Nanometer Films of Copper on Quartz and Silicon Substrate. Thin copper films on quartz substrate are obtained by direct photochemical deposition from the ethanol solutions of Cu(acac)₂, when a high fraction of light falls on the substrate surface and is absorbed by the solution–substrate interface. To

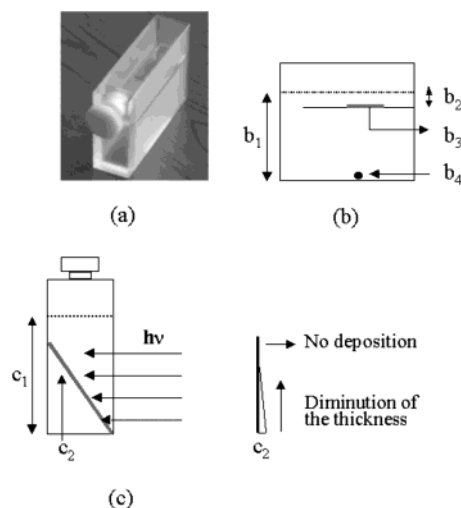


Figure 9. (a) Cuvette for deposition on opaque (silicon) substrates, irradiated from above. (b) Section of cuvette (a); b₁ solution level; b₂ solution thickness over the substrate; b₃ silicon substrate; b₄ stirrer. (c) Set up to make evident the filter effect of the thickness solution on film deposition.

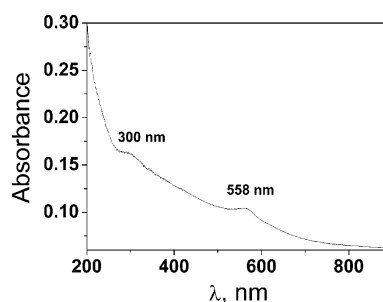


Figure 10. UV spectrum of metallic copper deposited on a quartz substrate.

realize this requisite, a suitable apparatus was used, in which the light irradiates from below the quartz substrate which is placed into the cuvette.¹⁸ The Cu 2p_{3/2} and Cu LMM XPS regions (Figure 4d) indicate that these films consist of metallic copper. SEM micrographs (Figure 8b) show the presence of grains with dimensions of about 80 nm. Also films of pure and homogeneous copper(0) have been obtained on silicon substrate. Deposition on an opaque substrate like Si requires a particular cuvette in which the irradiation has been performed from above (Figure 9a). Thickness and concentration of the solution have been selected to allow the light to reach the silicon substrate in order to establish if in the deposition mechanism a photochemical step is involved, as previously proposed; the following experiment has been performed. A silicon plate is placed along the diagonal of a 1-cm cuvette (Figure 9c) containing ethanol solution of Cu(acac)₂ 2.5×10^{-4} mol L⁻¹. After some hours of irradiation, a copper film is formed on the plate. The thickness decreases from the bottom to the top in parallel with the decreasing of the absorbed light. No deposition is observed when the light is completely absorbed by solution so that it does not reach the silicon surface.

This finding is consistent with the hypothesis of a photoinduced step of heterogeneous nature in the deposition process. The addition of a free ligand or acetone¹⁸ allows the use of lower energy (300 nm) and increases the photodeposition rate, without modification

(40) Hanglein, A. *J. Phys. Chem.* **1979**, *83*, 2209–2216.

(41) Paul, H.; Small, R. D. Scaiano, J. C., Jr. *J. Am. Chem. Soc.* **1978**, *100* (14), 4520–4527.

(42) Pischel, U.; Nau, W. M. *J. Am. Chem. Soc.* **2001**, *123* (40), 9727–9737.

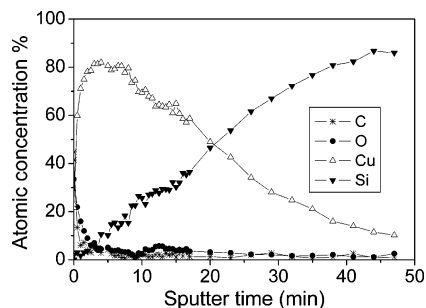


Figure 11. Typical XPS of films obtained on silicon by direct photochemical deposition.

of the film composition. For example, irradiation (300 nm) of solution containing $\text{Cu}(\text{acac})_2$, $5 \times 10^{-4} \text{ mol L}^{-1}$, and Hacac, $1 \times 10^{-3} \text{ mol L}^{-1}$, gives good films of metallic copper in about 2 h. In these conditions, the spectrum matches exactly the calculated absorption spectrum of 10-nm-diameter spherical particles in vacuo³⁹ (Figure 10).

The integrity of copper films has been evaluated by XPS depth profiles. A typical profile of films obtained on silicon by direct photochemical deposition is reported in Figure 11. No detectable carbon contamination (<2%) was observed in the bulk of the films, while oxygen content was lower than 5%. Similar results were obtained for films deposited on quartz substrates. Note that improved film quality was obtained in the presence of free Hacac ligand since neither oxygen (<1%) nor carbon were detected in the bulk.

Conclusions

The present paper highlights mechanistic aspects of a simple photochemical route for the formation of copper nanoparticles and for the fabrication of nanostructured films. The study of the photoreduction mechanism of this synthetic route shows that the formation of copper metal involves two consecutive steps, both of a photochemical nature. Therefore, the process rate can be easily controlled by light intensity.

The photochemical nature of both the reduction steps leading to nanosized copper represents a novel issue since previous literature data on the $\text{Cu}(\text{acac})_2$ photoreduction have reported on mixed processes to copper(0) involving a thermal dismutation.

The present pure photochemical process appears best suited for an accurate control of morphology as well as dimensions of both the powder and thin film by a fine-tuning of the irradiation condition. There is, therefore, evidence that photochemical deposition from $\text{Cu}(\text{acac})_2$ solutions represents a viable route for the fabrication of copper-based materials.

Acknowledgment. The authors thank the MIUR (Cofinanziamento di Programmi di Ricerca di Rilevante Interesse Nazionale e progetto FIRB 2001) for financial support. Authors thank Professor G. Condorelli and Professor S. Sortino for interesting and stimulating discussions.

CM034782H